JOC The Journal of Organic Chemistry

Article

pubs.acs.org/joc

Phthalimide Compounds Containing a Trifluoromethylphenyl Group and Electron-Donating Aryl Groups: Color-Tuning and Enhancement of Triboluminescence

Jun-ichi Nishida,*[,†] Hokuto Ohura,[‡] Yasuyuki Kita,[†] Hiroyuki Hasegawa,[‡] Takeshi Kawase,[†] Noriyuki Takada,[§] Hiroyasu Sato,[∥] Yoshihisa Sei,[⊥] and Yoshiro Yamashita[‡]

[†]Department of Applied Chemistry, Graduate School of Engineering, University of Hyogo, Himeji, Hyogo 671-2280, Japan

[‡]Department of Electronic Chemistry, Interdisciplinary Graduate School of Science and Engineering, Tokyo Institute of Technology, Yokohama, Kanagawa 226-8502, Japan

[§]Photonics Research Institute, National Institute of Advanced Industrial Science and Technology (AIST), Tsukuba, Ibaraki 305-8565, Japan

[∥]Rigaku Corporation , Tokyo 196-8666, Japan

[⊥]Material Analysis Suzukake-dai Center, Technical Department, Tokyo Institute of Technology, Yokohama, Kanagawa 226-8503, Japan

Supporting Information

ABSTRACT: Trifluoromethylphenyl-substituted phthalimide derivatives favorably form triboluminescence (TL) active noncentrosymmetric crystals. Oligothienyl-, oligophenyl-, and naphthyl-substituted phthalimide derivatives were successfully developed as a series of metal free TL compounds. X-ray crystal structure analyses of bithienyl and naphthyl derivatives revealed noncentrosymmetric layer structures in the same direction. Introduction of suitable electron rich π-units such as thienyl groups enhances their photoluminescence and TL characteristics, and the colors can be also controlled in the visible region. A rigid naphthyl-substituted imide derivative exhibits extremely high TL performance.

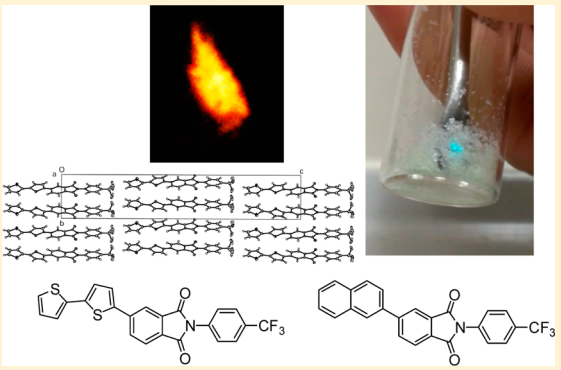

INTRODUCTION

Luminescence caused by mechanical excitation (motion or stress (force)) in solid materials is called as triboluminescence (TL) (mechanoluminescence (ML) as a broad sense). TL has a long history[1−3] and has recently been applied to real-time sensors of mechanical stress and structural damages,[4] light generators by using mechanical motion,[5] and a resource of X-ray.[6] As typical strong TL materials, there are some inorganic solids containing lanthanoids such as europium and their complexes.[1,7−9] Although organic π-conjugated compounds such as coumarin,[10] isopropyl carbazole,[11] and 9-anthracene carboxylic acid and the esters[12] also show TL, the reported numbers are limited, and the efficiency is generally low. TL mechanisms are dependent on compounds and still remain ambiguous.[13,14] To make them clear, further studies on the relationship between molecular structures and properties are essentially important. According to previous reports, TL performance is related to solid photoluminescence (PL) quantum yields and piezoelectric properties. Compounds showing TL usually have noncentrosymmetric molecular arrangements.[15] While noncentrosymmetric crystals can be obtained by introducing chiral units,[16] it is considered to be interesting and important for TL study to increase net dipole moments in the solids.[17] Recently, we have found that *N*-trifluoromethylphenyl-substituted phthalimide derivatives have a unique noncentrosymmetric layer structure and show vivid blue TL.[17] We are interested in the potential ability of the imides and have now introduced π-extended thienyl, phenyl, and naphthyl groups to the phthalimide core with a trifluoromethylphenyl group to give imide derivatives **I1**−**I6** shown in Figure 1 and succeeded in observing the TL properties. The compounds have the following advantages for TL properties. First, all derivatives form TL active noncentrosymmetric molecular crystals. The trifluoromethylphenyl phthalimide unit works as a trigger to create such crystals. Second, the extended π-systems increase the solid PL efficiency. Third, introduction of electron-donating π-systems affords intramolecular charge transfer (ICT)-type emission[18,19] based on imides, leading to color tunable TL. The increased dipole moments are also favorable for the piezoelectric properties. In this paper, their synthesis, crystal structures, and X-ray

Received: September 18, 2015
Published: December 11, 2015

DOI: 10.1021/acs.joc.5b02191
J. Org. Chem. 2016, 81, 433−441

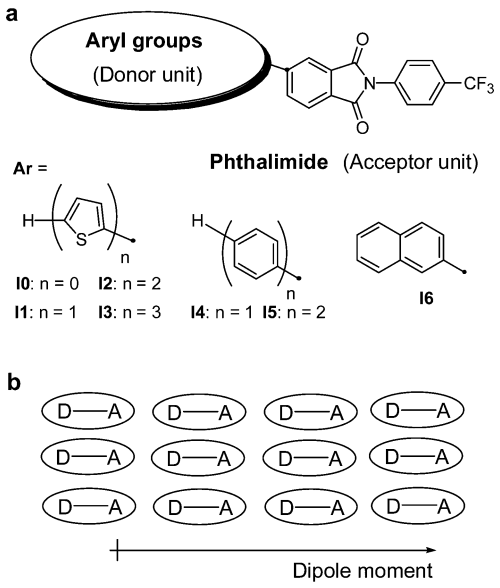

Figure 1. (a) D−A-type phthalimide compounds **I1**−**I6**. (b) A model of noncentrosymmetric TL active molecular arrangement with a direction of dipole moment.

diffraction (XRD) patterns and PL and TL properties are discussed.

RESULTS AND DISCUSSION

Synthesis. Thienyl-, phenyl-, biphenyl-, and naphthyl-substituted phthalimide derivatives **I1** and **I4**−**I6** were synthesized by the Stille coupling reaction of the corresponding aryl tin reagents with bromo-substituted phthalimide derivative **I7** (Scheme 1), which were prepared by a simple condensation

Scheme 1. Preparation of Imide Derivatives[a]

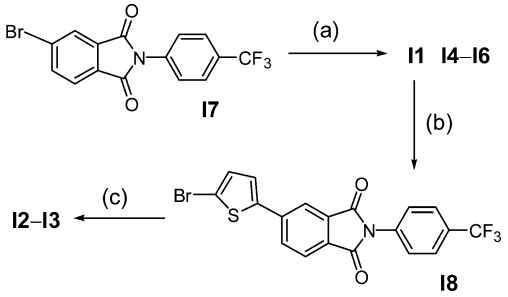

[a]Reagents (a) $Pd(PPh_3)_4$, tributyl(2-thienyl)stannane for **I1** (y. 40%), tributyl(phenyl)stannane for **I4** (31%), biphenyl-4-yl(tributyl)-stannane for **I5** (53%), tributyl(2-naphthyl)stannane for **I6** (57%); (b) NBS for **I8** (60%); (c) $Pd(PPh_3)_4$, tributyl(2-thienyl)stannane for **I2** (60%), 2,2′-bithienyl-5-yl(tributyl)stannane for **I3** (40%).

reaction of 4-(trifluoromethyl)aniline with bromo-substituted phthalic anhydrides (68%). [2,2′]Bithiophen-5-yl and [2,2′;5′,2″]terthiophen-5-yl derivatives **I2** and **I3** were prepared by the Stille coupling reaction of a brominated monothienyl phthalimide **I8**. These phthalimides have high thermal stability and could be purified by recrystallization and sublimation. The molecular orbital (MO) calculations of the imides were performed using RB3LYP/6-31G(d) levels, and the HOMOs, LUMOs, their energies, and dipole moments are summarized in Figure 2. The HOMOs are delocalized at the introduced aryl units, and the LUMOs are localized at the phthalimide core units. Elongation of π-units increases their dipole moments.

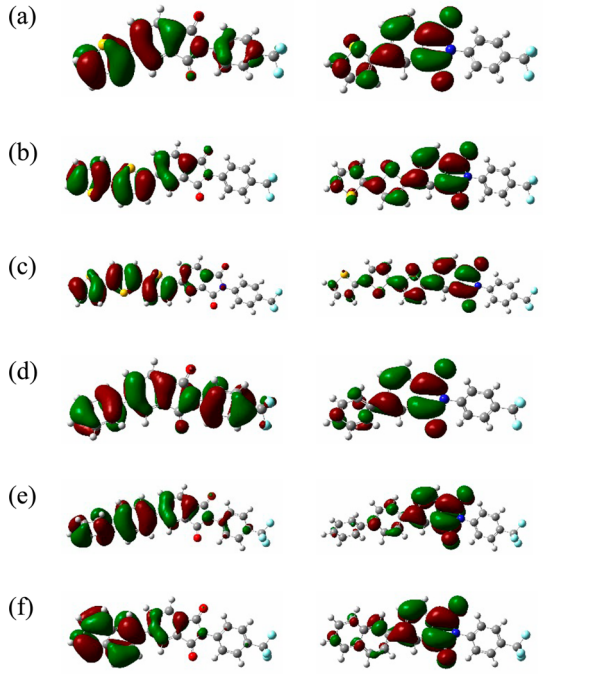

Figure 2. HOMO (left) and LUMO (right) of imides (a) **I1** (HOMO: −6.35, LUMO: −2.58 eV), (b) **I2** (−5.75, −2.63), (c) **I3** (−5.44, −2.65), (d) **I4** (−6.60, −2.50), (e) **I5** (−6.24, −2.50), and (f) **I6** (−6.14, −2.51) performed using Gaussian 09 at RB3LYP/6-31G(d) levels of theory. Dipole moments of the imides (**I1**: 6.58, **I2**: 7.43, **I3**: 7.92, **I4**: 6.63, **I5**: 7.06, **I6**: 7.00 debye) were also estimated.

X-ray Crystal Structure Analysis. Pale yellow single crystals of bithienyl-substituted imide **I2** and colorless single crystals of a naphthyl imide **I6** were obtained by slow evaporation of the chloroform/DMF or chloroform solution, respectively. Molecular structures of two imide derivatives **I2** and **I6** were clearly solved. X-ray analysis on **I2** revealed that the two independent molecules (molecule A and B) form a quite regular layer structure in the crystal as depicted in Figure 3, where they are arranged in the same direction with a noncentrosymmetric space group *Pn*. The oligothiophene and phthalimide parts are almost planar (maximum dihedral angle: 6.5°), and the units are packed in a herringbone manner with close contacts between the oxygens of imide units and the carbon atoms of the neighboring imide (C═O) units (the closest contact: 2.88 Å). Close C−H···π interactions between neighboring phthalimide units (2.73 Å) and between thienyl units (2.93 Å) are also observed. The trifluoromethylphenyl units are twisted to the phthalimide core planes with dihedral angles of 53.3° and 53.4°, respectively, and hydrogen atoms on them form hydrogen bonds (2.55 Å) with the oxygen atoms of the neighboring imide units leading to the noncentrosymmetric layer structure (Figure 3c).

On the other hand, two independent molecules (molecule A and B) were also observed in the crystal **I6** and form a quite similar noncentrosymmetric layer structure with a space group *Pc* as shown in Figure 4. The naphthyl and phthalimide parts are almost planar (maximum dihedral angle: 1.9°), and the units are packed in a herringbone manner. Similar close intermolecular contacts between the carbonyl units (the closest

DOI: 10.1021/acs.joc.5b02191
J. Org. Chem. 2016, 81, 433−441

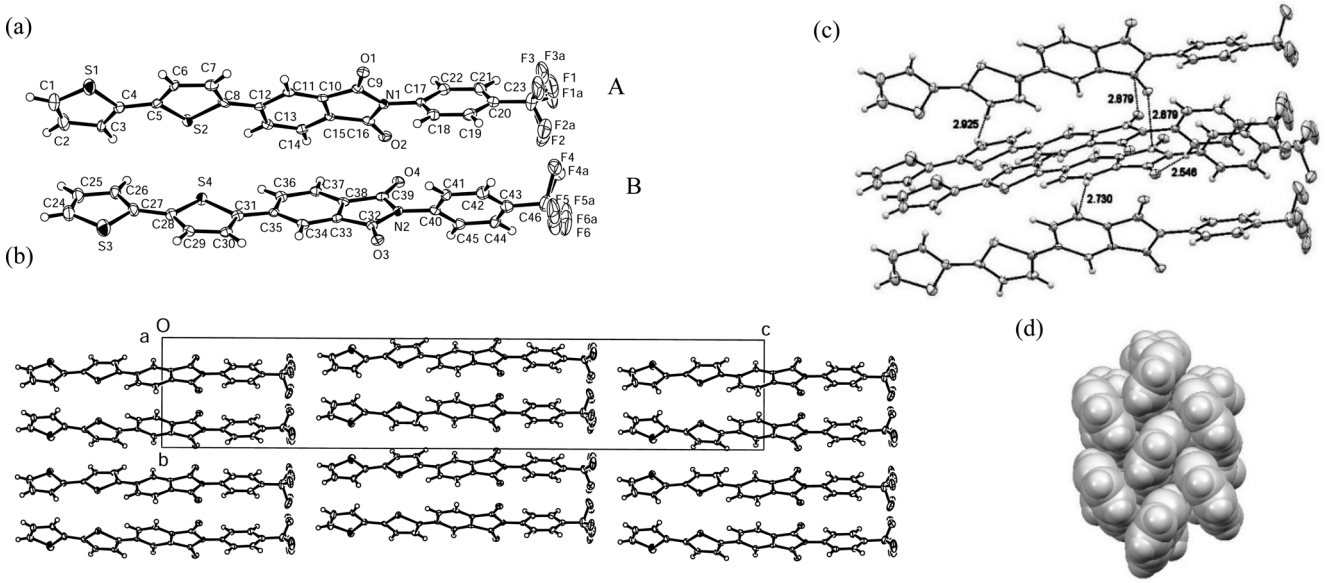

Figure 3. (a) Molecular structures of the bithienyl-substituted imide **I2** (50% probability). Two molecules A and B are independent. Fluorines in trifluoromethyl groups contain a rotational disorder. (b) The layer structure viewed along *a*-axis. (c) Close atom contacts. (d) Packing pattern of the thienyl side.

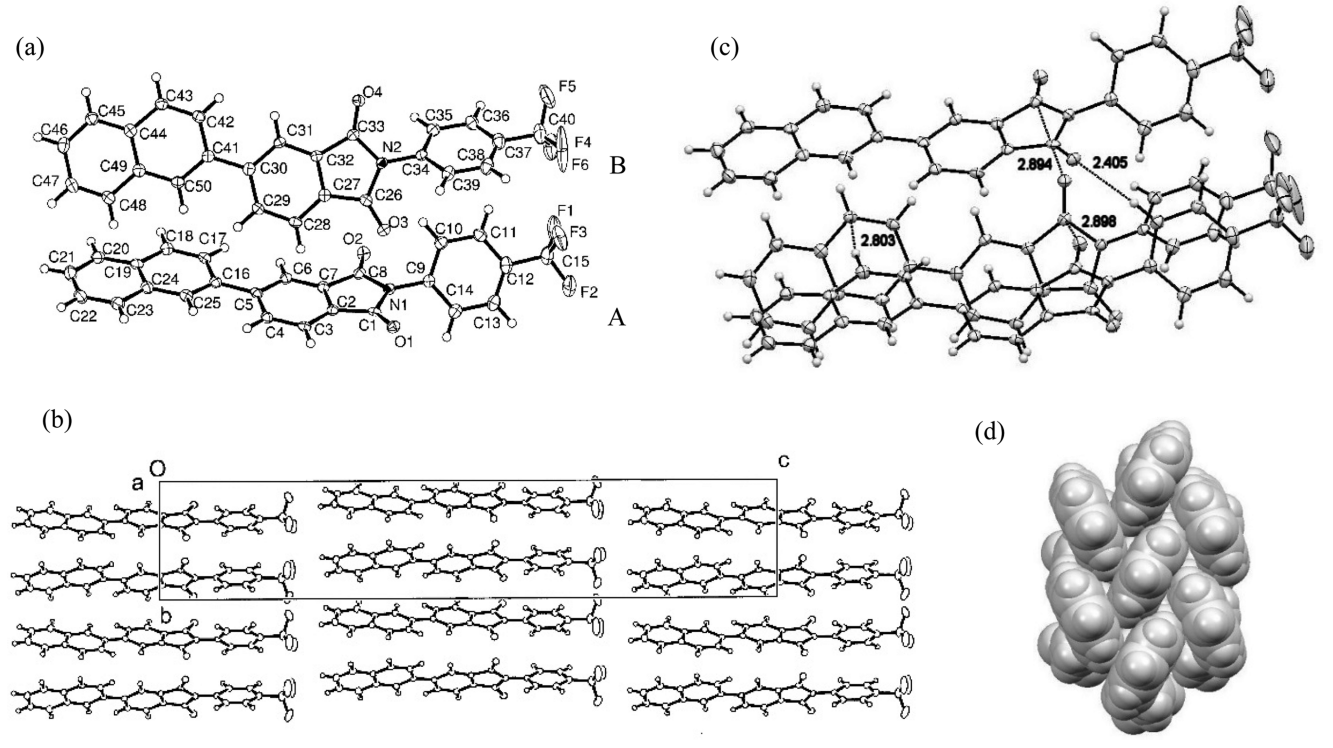

Figure 4. (a) Molecular structures of the naphthyl-substituted imide **I6** (50% probability). Two molecules A and B are independent. (b) The layer structure viewed along *a*-axis. (c) Close atom contacts. (d) Packing pattern of the naphthyl side.

contact: 2.89 Å) and C−H···π interactions between neighboring naphthyl units (2.80 Å) are observed. The trifluoromethylphenyl units are twisted to the phthalimide core planes with dihedral angles of 50.4° (both), and shorter hydrogen bonds (2.41 Å) are formed (Figure 4c), suggesting the strong molecular interaction in the crystal **I6**.

XRD Measurements. To investigate the molecular arrangements of imide derivatives, X-ray diffraction (XRD) patterns of powders were measured in a reflection mode and are shown in Figure 5. The XRD patterns based on thienyl-substituted **I1**−**I3** suggest that they have similar molecular arrangements. The *d*-spacings obtained from the first reflection peaks are 16.7 Å for **I1**, 20.3 Å for **I2**, and 24.9 Å for **I3**. Since the molecular lengths of the imides estimated from the MO calculations are 15.9 Å for **I1**, 19.8 Å for **I2**, and 23.7 Å for **I3**, respectively, these molecules are considered to form the similar noncentrosymmetric lamella structures corresponding to each molecular length. The similar layer structures are also formed in phenyl,

DOI: 10.1021/acs.joc.5b02191
J. Org. Chem. 2016, 81, 433−441

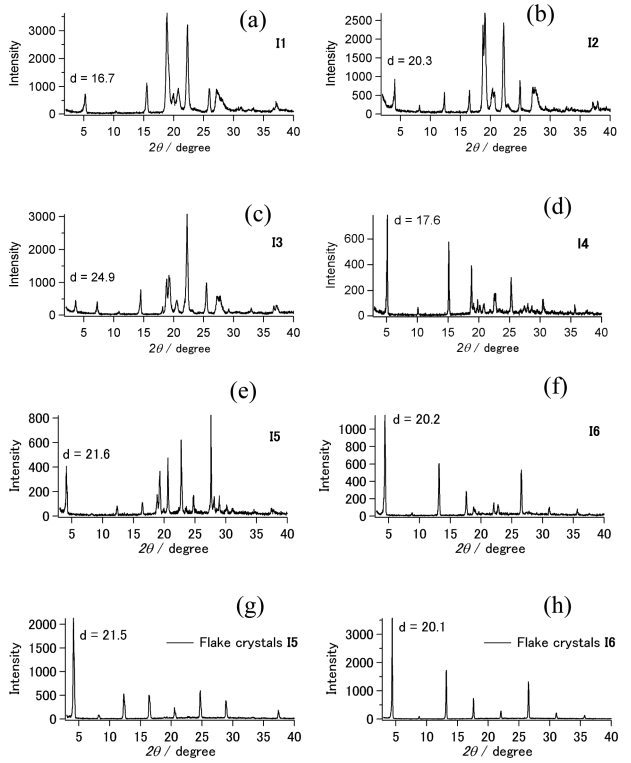

Figure 5. XRD patterns of powders (a) **I1**, (b) **I2**, (c) **I3**, (d) **I4**, (e) **I5**, and (f) **I6** and flake-type crystals (g) **I5** and (h) **I6**. The *d*-spacings based on the first reflection peaks were added for marks.

biphenyl, and naphthyl derivatives **I4**–**I6**. The *d*-spacings obtained from the first reflection peaks (17.6 Å for **I4**, 21.6 Å for **I5**, and 20.2 Å for **I6**) correspond to the calculated molecular lengths (16.0 Å for **I4**, 20.4 Å for **I5**, and 18.5 Å for **I6**). XRD patterns based on recrystallized flake-type crystals of **I5** and **I6** were also measured and added in Figure 5. They indicate that the lamellar ordered layer structures are formed into the vertical way of the flake crystals as seen in the structure analysis of **I6**.

Optical Properties. The colors and PL properties of phthalimides **I1**–**I6** are dependent on the introduced aryl units. In the solid state, thienyl-, bithienyl-, and terthienyl-substituted imides **I1**–**I3** are colorless, yellow, and reddish-orange, respectively (their diffuse reflectance spectra were added in the Supporting Information). These imide solids **I1**–**I3** exhibit blue (emission maximum: 430 nm), greenish-yellow (521 nm), and reddish-orange (598 nm) PL as shown in Figure 6a and Table 1. These results suggest that the solid PL colors can be controlled by the number of thiophene units. The solid PL

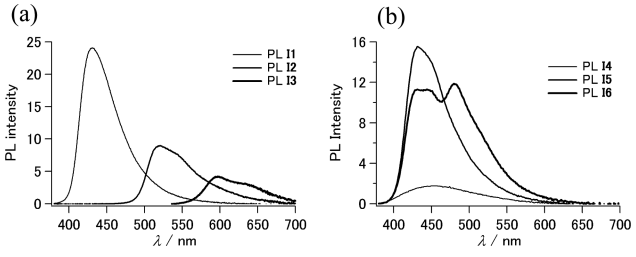

Figure 6. Solid PL spectra of (a) thienyl-, bithienyl-, and terthienyl-substituted imides **I1**–**I3** and (b) phenyl-, biphenyl-, and naphthyl-substituted imides **I4**–**I6**.

Table 1. Absorption and PL Data

		λ_{em}(nm) (Φ)		
compd	λ_{abs}(nm) (log ε)[a]	CH_2Cl_2[c]	CH_3CN[c]	solid[e]
I1	353 (3.55)	446 (0.50)	460 (0.57)	430 (0.27)
I2	351 (4.20), 400 (4.34)	552 (0.44)	591 (0.13)	521 (0.13)
I3	421[b]	–[f]	590 (0.03)	598 (0.06)
I4	254 (4.60), 321 (3.75)	445 (0.03)[d]	–[f]	456 (0.04)
I5	267 (4.51), 339 (4.11)	455 (0.44)	477 (0.52)	432 (0.22)
I6	255 (4.68), 363 (3.83) sh	463 (0.41)	500 (0.40)	431, 480 (0.25)
I0[g]	239 (4.48), 295 (3.22)	–[f]	–[f]	448 (0.04)

[a]In CH_2Cl_2. [b]Low solubility. [c]Estimated by using 9,10-diphenylanthracene (λ_{ex} = 366 nm, Φ = 0.90 in cyclohexane) as a standard.[20] [d]Estimated by using 2-phenyl benzoxazole (λ_{ex} = 299 nm, Φ = 0.75 in cyclohexane) as a standard.[21] [e]Integrating sphere (λ_{ex} = 366 nm). [f]Too weak to determine. [g]Ref 17.

efficiency can be also enhanced compared with the comparative compound **I0**. Introduction of a thienyl group increases contribution of ICT-type emission based on these imide compounds. Thus, when PL of **I2** was measured in dichloromethane and acetonitrile, a red-shift (ca. 39 nm) was observed in acetonitrile, and its PL quantum yield decreased (Figure 7 and Table 1).

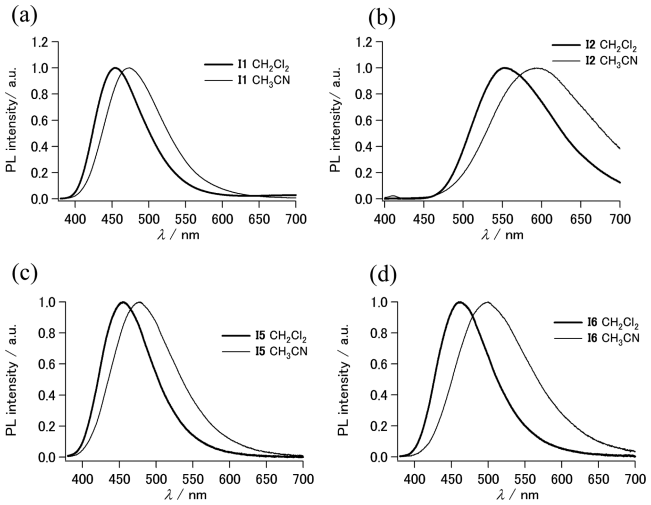

Figure 7. PL spectra of (a) monothienyl imide **I1**, (b) bithienyl imide **I2**, (c) biphenyl imide **I5**, and (d) naphthyl imide **I6** in dichloromethane and acetonitrile ($<10^{-5}$ M).

On the other hand, phenyl- and biphenyl-substituted imides **I4** and **I5** are different from imides **I1** and **I2**. Their solid colors are colorless, and the solid PL are observed in the blue region, suggesting that the contribution of the ICT is small. To explain the difference, the time-dependent density functional theory (TD-DFT) calculations were performed (Table 2 and the computational Supporting Information). The large oscillator strength based on the HOMO–LUMO transition of the imide **I2** (440 nm: f = 0.528) compared with that of **I5** (378 nm: f = 0.240) supports that the ICT from the bithienyl unit to the phthalimide core is effective. The PL quantum yield of the phenyl-substituted imide **I4** is considerably lower than that of the thienyl imide **I1**. The difference can be also explained by

DOI: 10.1021/acs.joc.5b02191
J. Org. Chem. 2016, 81, 433–441

Table 2. Selected Absorption Peaks of I1−I6 Calculated by TD-DFT Method[a]

	absorption, nm (oscillator strength: *f*)	assignments (ratios of contribution)
I1	378 (0.142)	HOMO → LUMO (66%)
	334 (0.091)	HOMO−1 → LUMO (65%)
I2	440 (0.528)	HOMO → LUMO (70%)
	355 (0.191)	HOMO → LUMO+1 (51%)
	353 (0.315)	HOMO−1 → LUMO (51%)
I3	491 (0.793)	HOMO → LUMO (70%)
	395 (0.666)	HOMO → LUMO+1 (69%)
	365 (0.015)	HOMO−1 → LUMO (63%)
	350 (0.105)	HOMO → LUMO+2 (60%)
I4	361 (0.043)	HOMO → LUMO (69%)
	328 (0.0007)	HOMO−4 → LUMO (69%)
	315 (0.147)	HOMO−1 → LUMO (66%)
I5	378 (0.240)	HOMO → LUMO (67%)
	342 (0.085)	HOMO−1 → LUMO (66%)
I6	389 (0.118)	HOMO → LUMO (69%)
	353 (0.006)	HOMO−1 → LUMO (67%)
	329 (0.011)	HOMO−4 → LUMO (64%)
	321 (0.092)	HOMO−2 → LUMO (59%)

[a]Calculated at the RB3LYP/6-31G(d) level of theory.

using TD-DFT calculations. The oscillator strength based on the HOMO−LUMO transition of **I4** (361 nm: f = 0.043) is smaller than that of **I1** (378 nm: f = 0.142). Instead, a large oscillator strength at 315 nm (f = 0.147) of **I4** is assigned to the transition from HOMO-1 to LUMO. The HOMO-1 of **I4** is mainly delocalized on the *N*-phenyl unit with twisted conformation as seen in the X-ray analyses of **I2** and **I6** (Figure 8). The electron transitions followed by conformation changes in the excited states are considered to lead to the low PL efficiency. In the case of the imide **I1**, the effective HOMO−LUMO transition results in the high PL property (Figure 8). Elongation of the phenyl group to the imide **I5** increases the biphenyl-side effective HOMO−LUMO transition

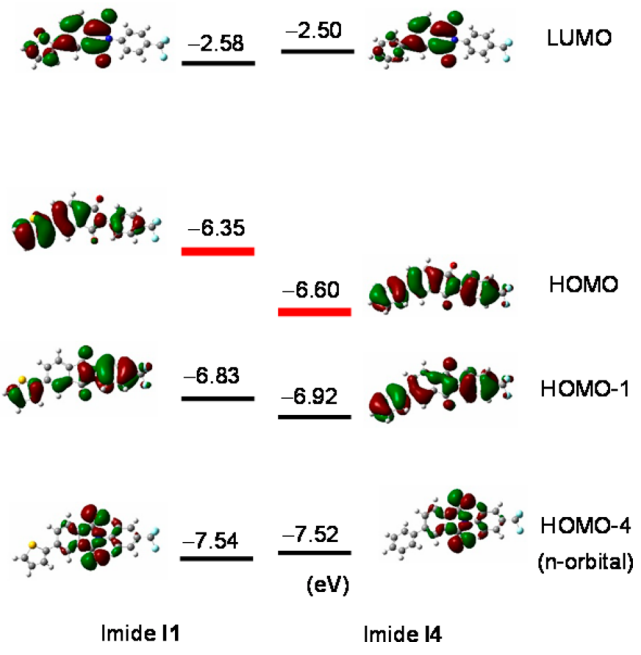

Figure 8. Molecular orbitals of imides **I1** and **I4**.

and enhances the PL efficiency. Introduction of the naphthyl group in **I6** is also effective to enhance the PL efficiency. The solid PL quantum yield increased to 0.25.

To investigate the optical properties in the solid states, the TD-DFT calculations were also performed by using the fixed molecular geometries in the Supporting Information CIF file of **I2** and Supporting Information CIF file of **I6** and are summarized in Table 3. From both the calculations of **I2** and

Table 3. TD-DFT Calculations of I2 and I6 Based on CIF Files[a]

	absorption, nm (oscillator strength: *f*)	assignments (ratios of contribution)
I2A	431 (0.651)	HOMO → LUMO (70%)
	352 (0.416)	HOMO → LUMO+1 (68%)
I2B	429 (0.616)	HOMO → LUMO (70%)
	352 (0.385)	HOMO → LUMO+1 (68%)
I6A	386 (0.181)	HOMO → LUMO (70%)
	341 (0.058)	HOMO−1 → LUMO (65%)
I6B	387 (0.184)	HOMO → LUMO (69%)
	344 (0.053)	HOMO−1 → LUMO (65%)

[a]Calculated at the RB3LYP/6-31G(d) level of theory.

I6, enhanced oscillator strengths based on the HOMO−LUMO transitions and blue-shifted absorption peaks were estimated. The large oscillator strengths indicate that the ICT states are also effective in the fixed planar geometries in the crystals.

Electrochemical Properties. The redox potentials of imides **I1−I3** were measured by cyclic voltammetry (CV). These derivatives showed a clear reversible reduction wave in DMF (E_{red} of **I1**: −1.21, **I2**: −1.17, **I3**: −1.17 V vs SCE) (Figure S5 in the Supporting Information). Their oxidation waves were observed as irreversible ones, and the potentials were obtained from the wave-onsets (E_{ox} of **I1**: +0.91, **I2**: +0.90, **I3**: +0.85 V vs SCE).

TL Experiments. Upon grinding with a spatula, imides **I1−I6** show TL. At room temperature, TL of imides **I1−I5** could be clearly caught by eyes in a darkish room (when the sample tube was cooled, the TL intensity drastically heightened). The TL data were collected outside the glass sample tubes through a plastic optical fiber to give the spectra (Figure 9). The TL peak maxima were observed at 454 nm (greenish-blue: strong) in **I1**, 576 nm (orange: strong) in **I2**, 587 nm (reddish-orange: weak) in **I3**, 440 nm (blue: strong) in **I4**, 471 nm (greenish-blue: strong) in **I5**, and 491 nm (light-blue: extremely strong) in **I6**, respectively. These TL suggest that the color can be tuned by introducing suitable π units to the phthalimide unit. Among them, the TL peak maxima in **I2** and **I5** were red-shifted compared to the original solid PL peaks (521 and 432 nm, respectively). The differences may be explained by considering the structural disorder on the solid surfaces caused upon grinding. The TL spectra are relatively consistent with the PL of "ground solids"[22] as shown in Figure 9. While the excited states are produced through electrification on the surface, the solid surfaces are broken to lead to amorphous states. More stable excited states can be produced through conformation changes or excimer formation in the amorphous solids.

On the other hand, it should be noted that the naphthyl-substituted imide **I6** shows extremely strong TL. Vivid light-blue TL of **I6** could be observed in daylight upon grinding at room temperature. We attribute the enhanced TL to the following effects. First, the imide **I6** has a high solid PL

DOI: 10.1021/acs.joc.5b02191
J. Org. Chem. 2016, 81, 433−441

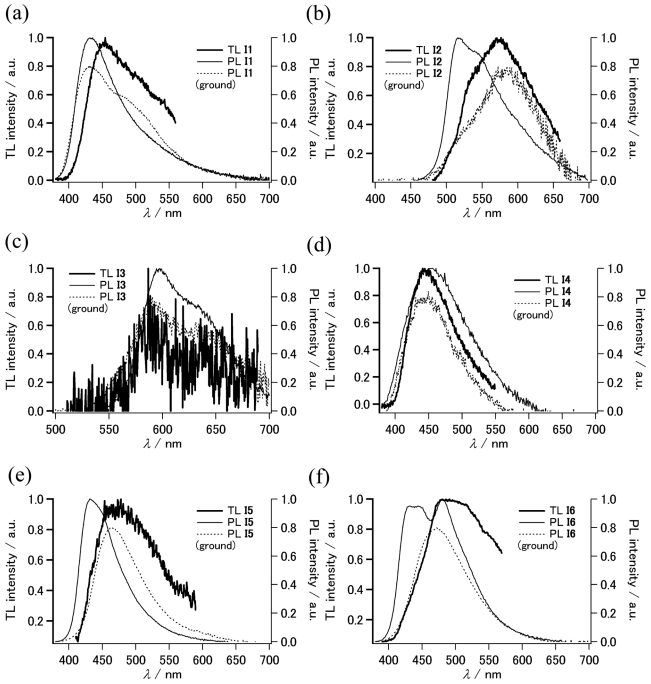

Figure 9. TL spectra of (a) **I1**, (b) **I2**, (c) **I3**, (d) **I4**, (e) **I5**, and (f) **I6**. PL spectra of solids and "ground solids" **I1**–**I6** were additionally added (as 100% and 80% relative intensity).

quantum yield among **I1**–**I6**. Second, its dipole moment is relatively high due to the electron-donating property of the naphthyl group. Third, the close C–H···π interactions and hydrogen bonds are observed in the X-ray structure analysis on **I6**. Such strong interactions are expected to lead to the effective electrification. The dense C–H···π packing of the rigid naphthyl units (Figure 4d) may suppress radiationless deactivation processes such as the rotation of naphthyl units. These results indicate that suitable rigid aryl substituents have an advantage in the enhancement of TL efficiency.

CONCLUSION

In this paper, we have developed oligothienyl-, oligophenyl-, and naphthyl-substituted phthalimide derivatives with a trifluoromethylphenyl group. These phthalimides derivatives form noncentrosymmetric molecular arrangements with the support of the trifluoromethylphenyl group and afford vivid TL. Introduction of suitable aryl units enhances their PL and TL properties, and their colors can be also tuned in the visible region. Such metal free organic TL materials may pioneer new application in stimuli response chemistry.[23,24] Further studies are now underway to apply these noncentrosymmetric TL active imide compounds to organic electronics.

EXPERIMENTAL SECTION

General Procedure. Tetrakis(triphenylphosphine)palladium(0): $Pd(PPh_3)_4$, *n*-butyllithium in *n*-hexane, tributyltin chloride, 5-bromoisobenzofuran-1,3-dione (4-bromophthalic anhydride), 4-(trifluoromethyl)aniline, tributyl(2-thienyl)stannane, and DMF were purchased and used without further purification. NMR spectrometers and the chemical shifts were referenced to tetramethylsilane (TMS). PL quantum yields in the solid state were determined by using an integrating sphere. XRD measurements were carried out with a CuKα source (λ = 1.541 Å). Cyclic voltammograms were measured by using a Pt disk working electrode, a Pt wire counter, and a SCE reference electrode. Tetrabutylammonium hexafluorophosphate ($TBAPF_6$: 0.1 mol dm^{-3}) was used as a supporting electrolyte in dry dichloromethane.

Computational Studies. Calculations were carried out using Chem3D Pro 7.0 and Gaussian 09.[25] The structures of imides were first optimized by the MM2 level of theory implemented in Chem3D (the constants used for MM2 are shown in the computational Supporting Information). From the structures, the molecular geometries were again optimized by the semiempirical calculation using RPM3 method implemented in Gaussian 09. From the structures, the ground-state geometries were finally optimized in the gas phase by DFT using the RB3LYP functional and 6-31G(d) basis set with Gaussian 09. The MO calculations are performed without conformational restraint. With the geometries, TD-DFT calculations were carried with Gaussian 09 at the same level of theory (Table 2). On the other hand, the MO energy calculations on **I2** (independent molecules: A and B) and **I6** (independent molecules: A and B) were also carried out by using the fixed molecular geometries in the CIF files (Table 3) (the HOMOs and LUMOs are shown in the computational Supporting Information). Minor fluorine atoms at the disordered CF_3 units of **I2** are omitted.

Synthesis of 5-Bromo-2-(4-trifluoromethylphenyl)-isoindole-1,3-dione (Imide I7). A mixture of 4-bromophthalic anhydride (6.38 g, 28.0 mmol) and 4-trifluoromethylaniline (4.54 g, 28.0 mmol) in dry DMF (70 mL) was refluxed for 24 h under N_2. After cooling to room temperature, the resulting precipitates were collected by suction and washed with methanol. Recrystallization from DMF gave a pale yellow solid of **I7** (7.07 g) in 68% yield. Mp 233–234 °C. ^{1}H NMR (500 MHz, $CDCl_3$, 20 °C) δ = 8.12 (d, 1H, J = 1.5 Hz), 7.97 (dd, 1H, J = 8.2, 1.5 Hz), 7.85 (d, 1H, J = 8.2 Hz), 7.78 (AA′XX′, 2H, J = 8.5 Hz), 7.63 (AA′XX′, 2H, J = 8.5 Hz). ^{13}C NMR (125 MHz, DMSO, 25 °C) δ = 166.0 (1C, C=O), 165.4 (1C, C=O), 137.6 (1C), 135.4 (1C), 133.6 (1C), 130.5 (1C), 128.4 (1C), 128.1 (1C, quartet, J = 32.5 Hz, **C**(Ph)-CF_3), 127.8 (2C), 126.5 (1C), 126.0 (2C, m, **C**(Ph)-C-CF_3), 125.4 (1C), 124.0 (1C, quartet, J = 270 Hz, **C**F_3). IR(KBr) ν max/cm^{-1} 3068, 1721 (C=O), 1417, 1399, 1341, 1171, 1119, 1097, 1070, 838, 735. Anal. calcd for $C_{15}H_7BrF_3NO_2$: C, 48.68; H, 1.91; N, 3.78. Found: C, 48.62; H, 1.71; N 3.80.

Synthesis of 5-Thiophen-2-yl-2-(4-trifluoromethylphenyl)-isoindole-1,3-dione (Imide I1). A mixture of imide **I7** (3.69 g, 10.0 mmol, tributyl(2-thienyl)stannane (3.76 g, 10.1 mmol) and $Pd(PPh_3)_4$ (0.470 g, 0.407 mmol) in toluene (100 mL) was refluxed for 24 h under Ar After cooling in an ice bath, and he resulting solid was collected by suction. Recrystallization of the crude product from DMF gave a colorless solid of imide **I1** (1.50 g, 4.02 mmol) in 40% yield. Mp 266–267 °C. MS/EI (70 eV): m/z 373 (M^+, 100). ^{1}H NMR (300 MHz, DMSO-d_6, 20 °C): δ (ppm) 8.25 (s, 1H), 8.16 (d, 1H, J = 8.1 Hz), 8.01 (d, 1H, J = 8.1 Hz), 7.94–7.91 (m, 3H), 7.77–7.72 (m, 3H), 7.24 (dd, J = 4.8, 3.3 Hz, 1H). ^{13}C NMR (125 MHz, $CDCl_3$, 20 °C) δ = 166.6 (1C, C=O), 166.4 (1C, C=O), 141.7 (1C), 141.2 (1C), 134.9 (1C), 132.6 (1C), 131.4 (1C), 129.9 (1C, quartet, J = 33.8 Hz, **C**(Ph)-CF_3), 129.4 (1C), 128.8 (1C), 127.7 (1C), 126.4 (2C), 126.3 (2C, quartet, J = 3.8 Hz, **C**(Ph)-C-CF_3), 125.8 (1C), 124,7 (1C), 123.8 (1C, quartet, J = 275 Hz, **C**F_3), 120.7 (1C). IR(KBr) ν max/cm^{-1} 3133, 3079, 1781, 1719 (C=O), 1616, 1401, 1116, 1339, 741, 711. Anal. calcd for $C_{19}H_{10}F_3NO_2S$: C, 61.12; H, 2.70; N, 3.75; S, 8.59. Found: C, 61.27; H, 2.71; N 3.81; S, 8.56.

Synthesis of 5-(5-Bromo-thiophen-2-yl)-2-(4-trifluoromethylphenyl)-isoindole-1,3-dione (Imide I8). To a solution of imide **I1** (1.00 g, 2.68 mmol) in DMF (20 mL) was added very slowly a solution of *N*-bromosuccinimide (1.00 g, 5.64 mmol) in DMF (8 mL) at 70 °C. The reaction mixture was stirred for 24 h at 70 °C. After cooling to room temperature, the reaction mixture was poured onto ice bath, and the resultant precipitates were collected by suction. Purification by recrystallization from DMF gave the imide **I8** (0.725 g, 60%) as a white solid. Mp 229–231 °C. MS/EI (70 eV): m/z 453 (M^+, 36), 451 (M^+, 34), 373 (M^+ − Br, 100). ^{1}H NMR (300 MHz, DMSO-d_6, 25 °C): δ (ppm) 8.23 (br. s, 1H), 8.09 (dd, 1H, J = 7.1, 1.8 Hz), 8.00 (d, 1H, J = 7.1 Hz), 7.93 (AA′XX′, 2H, J = 9.0 Hz), 7.79 (d, 1H, J = 5.2 Hz), 7.73 (AA′XX′, 2H, J = 9.0 Hz), 7.38 (d, 1H, J = 5.2 Hz). ^{13}C NMR (125 MHz, $CDCl_3$, 20 °C) δ = 166.4 (1C, C=O),

DOI: 10.1021/acs.joc.5b02191
J. Org. Chem. 2016, 81, 433–441

166.2 (1C, C═O), 143.0 (1C), 140.2 (1C), 134.8 (1C), 132.7 (1C), 131.6 (1C), 129.9 (1C, quartet, J = 32.5 Hz, **C**(Ph)-CF_3), 129.7 (1C), 126.4 (2C), 126.2 (2C, quartet, J = 3.8 Hz, **C**(Ph)-C-CF_3), 126.0 (1C), 124,9 (1C), 123.8 (1C, quartet, J = 272 Hz, **C**F_3), 120.3 (1C), 114.9 (1C). IR(KBr) ν max/cm^{-1} 3082, 1783, 1716 (C═O), 1615, 1393, 1119, 1334, 742, 711. Anal. calcd for $C_{19}H_9BrF_3NO_2S$: C, 50.46; H, 2.01; N, 3.10. Found: C, 50.38; H, 1.86; N 3.08.

Synthesis of 5-[2,2′]Bithiophenyl-5-yl-2-(4-trifluoromethylphenyl)-isoindole-1,3-dione (Imide I2). A mixture of imide **I7** (1.01 g, 2.23 mmol), tributyl(2-thienyl)stannane (836 mg, 2.24 mmol) and $Pd(PPh_3)_4$ (0.110 g, 95.2 μmol) in dry toluene (30 mL) was refluxed for 24 h. After cooling in an ice bath, the resulting precipitates were collected by suction. Recrystallization from DMF followed by sublimation gave a yellow solid of imide **I2** (610 mg, 1.33 mmol) in 60% yield. Mp 291−294 °C. MS/EI (70 eV): m/z 455 (M^+, 100). ^{1}H NMR (400 MHz, DMSO-d_6, 25 °C): δ (ppm) 8.28 (d, 1H, J = 1.2 Hz), 8.17 (dd, 1H, J = 8.0, 1.2 Hz), 8.02 (d, 1H, J = 8.0 Hz), 7.95 (AA′XX′, 2H, J = 8.4 Hz), 7.95 (d, 1H, J = 4.0 Hz), 7.75 (AA′XX′, 2H, J = 8.4 Hz), 7.61 (dd, 1H, J = 4.8, 1.2 Hz), 7.46 (dd, 1H, J = 3.6, 1.2 Hz), 7.45 (d, 1H, J = 4.0 Hz), 7.16 (dd, 1H, J = 4.8, 3.6 Hz). IR(KBr) ν max/cm^{-1} 3116, 3070, 1787, 1717 (C═O), 1615, 1399, 1117, 1335, 739, 699. Anal. calcd for $C_{23}H_{12}F_3NO_2S_2$: C, 60.65; H, 2.66; N, 3.08; S, 14.08. Found: C, 60.68; H, 2.67; N, 3.08; S, 14.09. ^{13}C NMR could not be measured for the solubility.

Synthesis of 5-[2,2′;5′,2″]Terthiophen-5-yl-2-(4-trifluoromethylphenyl)-isoindole-1,3-dione (Imide I3). A mixture of imide **I8** (2.04 g, 3.50 mmol), [2,2′]bithiophen-5-yl(tributyl)stannane[26] (1.59 g, 3.50 mmol), and $Pd(PPh_3)_4$ (202 mg, 0.180 mmol) in toluene (30 mL) was refluxed for 24 h under Ar. After cooled to room temperature, the resulting precipitates were collected by suction. Purification by sublimation gave a red solid of the imide **I3** (754 mg) in 40% yield. Mp 331−334 °C. MS/EI (70 eV): m/z 537 (M^+, 100). IR(KBr) ν max/cm^{-1} 3137, 3064, 1716 (C═O), 1615, 1398, 1120, 1339, 739, 702. Anal. calcd for $C_{27}H_{14}F_3NO_2S_3$: C, 60.32; H, 2.62; N, 2.61; S, 17.89. Found: C, 60.59; H, 2.57; N, 2.61; S, 18.17. ^{1}H and ^{13}C NMR could not be measured for the solubility.

Synthesis of 5-Phenyl-2-(4-trifluoromethylphenyl)-isoindole-1,3-dione (Imide I4). A mixture of imide **I7** (3.70 g, 10.0 mmol), tributyl(phenyl)stannane (4.42 g, 12.0 mmol), and $Pd(PPh_3)_4$ (580 mg, 0.502 mmol) in dry toluene (100 mL) under Ar was refluxed for 24 h. After cooling in an ice bath, the resulting precipitates were collected by suction. Recrystallization from DMF gave a colorless solid of **I4** (1.15 g, 3.13 mmol) in 31% yield. Mp 236−237 °C. ^{1}H NMR (500 MHz, $CDCl_3$, 20 °C) δ = 8.20 (d, 1H, J = 1.0 Hz), 8.04 (br. m, 2H), 7.79 (AA′XX′, 2H, J = 8.5 Hz), 7.69−7.66 (m, 3H), 7.54 (dd, 2H, J = 7.0, 7.0 Hz), 7.48 (br. t, 1H, J = 7.0 Hz). ^{13}C NMR (125 MHz, $CDCl_3$, 20 °C) δ = 166.8 (1C, C═O), 166.7 (1C, C═O), 148.3 (1C), 138.8 (1C), 135.0 (1C), 133.3 (1C), 132.4 (1C), 129.8 (1C), 129.8 (1C, quartet, J = 32.5 Hz, **C**(Ph)-CF_3), 129.3 (2C), 129.1 (1C), 127.4 (2C), 126.4 (2C), 126.2 (2C, m, **C**(Ph)-C-CF_3), 124.5 (1C), 123.8 (1C, quartet, J = 271 Hz, **C**F_3), 122.5 (1C). MS (FAB): m/z 367 (M^+). IR(KBr) ν max/cm^{-1} 3090, 1718 (C═O), 1616, 1398, 1341, 1170, 1117, 1070, 837, 768, 737. Anal. calcd for $C_{21}H_{12}F_3NO_2$: C, 68.67; H, 3.29; N, 3.81. Found: C, 68.70; H, 3.29; N 3.81.

Synthesis of 5-(4-Phenylphenyl)-2-(4-trifluoromethylphenyl)-isoindole-1,3-dione (Imide I5). A mixture of imide **I7** (3.69 g, 10.0 mmol), biphenyl-4-yl(tributyl)stannane[27] (6.65 g, 15.0 mmol), and $Pd(PPh_3)_4$ (420 mg, 0.363 mmol) in dry toluene (100 mL) was refluxed for 24 h under Ar. After cooling in an ice bath, the resulting precipitates were collected by suction. Recrystallization from DMF and purification by sublimation gave a colorless solid of **I5** (2.35 g, 5.29 mmol) in 53% yield. Mp 306−309 °C. ^{1}H NMR (500 MHz, $CDCl_3$, 20 °C) δ = 8.25 (s, 1H), 8.09 (d, 1H, J = 8.0 Hz), 8.06 (d, 1H, J = 8.0 Hz), 7.81−7.77 (m, 6H), 7.69−7.66 (m, 4H), 7.51−7.48 (m, 2H), 7.41 (br. t, 1H, J = 7.2 Hz). MS (FAB): m/z 443 (M^+). IR(KBr) ν max/cm^{-1} 3090, 1719 (C═O), 1398, 1341, 1170, 1119, 1071, 835, 743. Anal. calcd for $C_{27}H_{16}F_3NO_2$: C, 73.13; H, 3.64; N, 3.16. Found: C, 73.21; H, 3.51; N 3.19. ^{13}C NMR could not be assigned.

Synthesis of 5-(Naphthalen-2-yl)-2-(4-trifluoromethylphenyl)-isoindole-1,3-dione (Imide I6). A mixture of imide **I7** (2.97 g, 8.01 mmol), tributyl(naphthalen-2-yl)stannane[28] (4.25 g, 10.2 mmol), and $Pd(PPh_3)_4$ (390 mg, 0.337 mmol) in dry toluene (100 mL) was refluxed for 24 h under Ar. After cooling to room temperature, toluene was evaporated. The reaction mixture was triturated with methanol, and the resulting solid was filtrated. Purification by sublimation gave a pale yellow solid of **I6** (1.92 g, 4.60 mmol) in 57% yield. Mp 260−262 °C. ^{1}H NMR (500 MHz, $CDCl_3$, 20 °C) δ = 8.33 (d, 1H, J = 1.5 Hz), 8.18−8.16 (m, 2H), 8.08 (d, 1H, J = 8.0 Hz), 8.01 (d, 1H, J = 8.0 Hz), 7.97−7.95 (m, 1H), 7.93−7.91 (m, 1H), 7.81−7.79 (m, 3H), 7.68 (AA′XX′, 2H, J = 8.5 Hz), 7.59−7.56 (m, 2H). ^{13}C NMR (125 MHz, $CDCl_3$, 40 °C) δ = 166.8 (1C, C═O), 166.7 (1C, C═O), 148.4 (1C), 136.1 (1C), 135.2 (1C), 133.6 (1C), 133.51 (1C), 133.47 (1C), 132.6 (1C), 129.95 (1C, quartet, J = 32.5 Hz, **C**(Ph)-CF_3), 129.97 (1C), 129.3 (1C), 128.5 (1C), 127.8 (1C), 127.1 (1C), 126.99 (1C), 126.97 (1C), 126.5 (2C), 126.3 (2C, m, **C**(Ph)-C-CF_3), 124.8 (1C), 124.6 (1C), 123.9 (1C, quartet, J = 270 Hz, **C**F_3), 122.8 (1C). MS (FAB): m/z 417 (M^+). IR(KBr) ν max/cm^{-1} 3062, 1718 (C═O), 1614, 1401, 1340, 1167, 1117, 1070, 832, 818, 753. Anal. calcd for $C_{25}H_{14}F_3NO_2$: C, 71.94; H, 3.38; N, 3.36. Found: C, 72.10; H, 3.30; N 3.38.

X-ray Crystal Structure Analysis. X-ray measurements of single crystals of **I2** and **I6** were made on a Rigaku R-AXIS RAID diffractometer using multilayer mirror monochromated Cu-Kα radiation (λ = 1.54187 Å) at −180 °C. The structures were solved by the direct methods (SIR2008 for **I2** and SHELXT Version 2014/4[29] for **I6**) and refined by the full-matrix least-squares method on F^2. The non-hydrogen atoms were refined anisotropically. Hydrogen atoms were refined using the riding model. Absorption corrections were applied using an empirical procedure. All calculations were performed using the CrystalStructure crystallographic software package except for refinements, which were performed using SHELXL-97[30] for **I2** and SHELXL Version 2014/7 for **I6**.[30] Crystal data for **I2**: a yellow block crystal, $C_{23}H_{12}F_3NO_2S_2$, M_r = 455.47, crystal dimensions 0.13 × 0.10 × 0.08 mm, monoclinic, space group Pn, a = 5.7685(3), b = 7.7643(5), c = 42.476(2) Å, β = 91.849(7), V = 1901.4(2) Å^3, Z = 4, D_c = 1.591 g cm^{-3}, 12495 reflections collected, 5611 independent (R_{int} = 0.0359), GOF = 0.979, R_1 = 0.0417 (I > 2.00 $\sigma(I)$), wR_2 = 0.1031 for all reflections. Flack parameter 0.029(16) (Friedel pairs = 2186). CCDC number is 970311. Crystal data for **I6**: a colorless prism crystal, $C_{25}H_{14}F_3NO_2$, M_r = 417.39, crystal dimensions 0.31 × 0.22 × 0.15 mm, monoclinic, space group Pc, a = 5.90211(11), b = 7.66146(14), c = 40.2458(7) Å, β = 93.335(7), V = 1816.78(6) Å^3, Z = 4, D_c = 1.526 g cm^{-3}, 12028 reflections collected, 5373 independent (R_{int} = 0.0347), GOF = 1.089, R_1 = 0.0404 (I > 2.00 $\sigma(I)$), wR_2 = 0.1162 for all reflections. Flack parameter −0.02(8) (Parsons' quotients = 1741). CCDC number is 1438175.

TL Measurements. TL spectra were measured with a polychrometor-ICCD multichannel spectrophotometer system (Princeton Instruments Inc.) through a plastic optical fiber. The powder samples were continuously ground in the glass sample tubes with a stainless spatula during the measurements as shown in Figure 10. A light detection period was 500 ms, and the data were accumulated 30 times to depict the spectra. The spectra were drawn by deducting the blank spectra. The measurements were carried out at room temperature except for that of the terthienyl-substituted imide **I3**. In the case of **I3**, once the solid in the tube was cooled in a liquid nitrogen bath, the sample was pulled out from the bath and immediately ground.

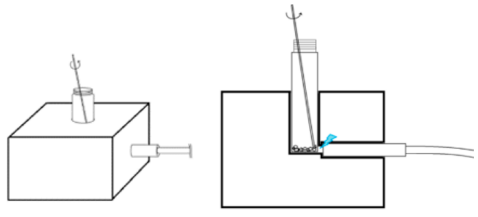

Figure 10. An illustration of the TL measurement. A black colored foamed polystyrene case was used as a support.

DOI: 10.1021/acs.joc.5b02191
J. Org. Chem. 2016, 81, 433−441

Transient properties of TL were also monitored by a photomultiplier connected to a storage oscilloscope (HP 54542A).

■ ASSOCIATED CONTENT

Supporting Information

The Supporting Information is available free of charge on the ACS Publications website at DOI: 10.1021/acs.joc.5b02191.

UV−vis spectra of imides **I1**−**I6**, diffuse reflectance spectra of **I1**−**I6**, XRD patterns of ground solids of **I1**−**I6**, cyclic voltammograms of **I1**−**I3**, transient property of TL of **I1** and **I2**, NMR and FT-IR spectra of **I1**−**I6** (PDF)

DFT and TD-DFT calculations of imides **I1**−**I6** (PDF)

Crystallographic data for **I6** (CIF)

Crystallographic data for**I2** (CIF)

(PDF)

(PDF)

■ AUTHOR INFORMATION

Corresponding Author

*E-mail: jnishida@eng.u-hyogo.ac.jp.

Notes

The authors declare no competing financial interest.

■ ACKNOWLEDGMENTS

This work is financially supported by a Grant-in-Aid for Scientific Research on Innovation Areas "Stimuli-responsive Chemical Species" (nos. 25109515 and 15H00959), Scientific Research (B) (no. 23350088), Scientific Research (C) (no. 25410209) from the Ministry of Education, Culture, Sports, Science and Technology (MEXT), Japan. We thank Materials Analysis Suzukake-dai Center, Technical Department, Tokyo Institute of Technology, for elemental analysis and MS measurements.

■ REFERENCES

(1) Hurt, C. R.; McAvoy, N.; Bjorklund, S.; Filipescu, N. *Nature* **1966**, *212*, 179−180.

(2) (a) Zink, J. I. *Acc. Chem. Res.* **1978**, *11*, 289−295. (b) Zink, J. I. *Naturwissenschaften* **1981**, *68*, 507−512.

(3) (a) Hardy, G. E.; Baldwin, J. C.; Zink, J. I.; Kaska, W. C.; Liu, P.-H.; Dubois, L. *J. Am. Chem. Soc.* **1977**, *99*, 3552−3558. (b) Chandra, B. P.; Zink, J. I. *J. Phys. Chem.* **1982**, *86*, 4138−4141.

(4) (a) Sage, I.; Bourhill, G. *J. Mater. Chem.* **2001**, *11*, 231−245. (b) Sage, I.; Badcock, R.; Humberstone, L.; Geddes, N.; Kemp, M.; Bourhill, G. *Smart Mater. Struct.* **1999**, *8*, 504−510.

(5) Jeong, S. M.; Song, S.; Lee, S.-K.; Choi, B. *Appl. Phys. Lett.* **2013**, *102*, 051110.

(6) Camara, C. G.; Escobar, J. V.; Hird, J. R.; Putterman, S. J. *Nature* **2008**, *455*, 1089−1092.

(7) Zhan, T. Z.; Xu, C.-N.; Yamada, H.; Terasawa, Y.; Zhang, L.; Iwase, H.; Kawai, M. *Appl. Phys. Lett.* **2012**, *100*, 014101.

(8) (a) Takada, N.; Sugiyama, J.; Katoh, R.; Minami, N.; Hieda, S. *Synth. Met.* **1997**, *91*, 351−354. (b) Takada, N.; Hieda, S.; Sugiyama, J.; Katoh, R.; Minami, N. *Synth. Met.* **2000**, *111*, 587−590. (c) Li, D.-P.; Li, C.-H.; Wang, J.; Kang, L.-C.; Wu, T.; Li, Y.-Z.; You, X.-Z. *Eur. J. Inorg. Chem.* **2009**, *2009*, 4844−4849.

(9) (a) Rheingold, A. L.; King, W. *Inorg. Chem.* **1989**, *28*, 1715−1719. (b) Clegg, W.; Sage, I.; Oswald, I.; Brough, P.; Bourhill, G. *Acta Crystallogr., Sect. C: Cryst. Struct. Commun.* **2000**, *56*, 1323−1325.

(10) Zink, J. I.; Klimt, W. *J. Am. Chem. Soc.* **1974**, *96*, 4690−4692.

(11) (a) Nowak, R.; Krajewska, A.; Samoć, M. *Chem. Phys. Lett.* **1983**, *94*, 270−271. (b) Tsuboi, Y.; Seto, T.; Kitamura, N. *J. Phys. Chem. B* **2003**, *107*, 7547−7550.

(12) Sweeting, L. M.; Rheingold, A. L.; Gingerich, J. M.; Rutter, A. W.; Spence, R. A.; Cox, C. D.; Kim, T. J. *Chem. Mater.* **1997**, *9*, 1103−1115.

(13) Sweeting, L. M. *Chem. Mater.* **2001**, *13*, 854−870.

(14) Tsuboi, Y.; Seto, T.; Kitamura, N. *J. Phys. Chem. A* **2008**, *112*, 6517−6521.

(15) There are some examples of centrosymmetric crystalline materials showing TL as reported in ref 9a.

(16) A successful example is anthracene derivatives with chiral esters reported in ref 12.

(17) Nakayama, H.; Nishida, J.-i.; Takada, N.; Sato, H.; Yamashita, Y. *Chem. Mater.* **2012**, *24*, 671−676. In the paper, trifluoromethylphenyl-substituted phthalimides with large net dipole moments show the higher TL properties than a methylphenyl-substituted imide with a small one.

(18) (a) Colvin, M. T.; Ricks, A. B.; Scott, A. M.; Co, D. T.; Wasielewski, M. R. *J. Phys. Chem. A* **2012**, *116*, 1923−1930. (b) Bhosale, S. V.; Jani, C. H.; Langford, S. J. *Chem. Soc. Rev.* **2008**, *37*, 331−342. (c) Hains, A. W.; Liang, Z.; Woodhouse, M. A.; Gregg, B. A. *Chem. Rev.* **2010**, *110*, 6689−6735. (d) Sakai, N.; Mareda, J.; Vauthey, E.; Matile, S. *Chem. Commun.* **2010**, *46*, 4225−4237.

(19) Wakita, J.; Sekino, H.; Sakai, K.; Urano, Y.; Ando, S. *J. Phys. Chem. B* **2009**, *113*, 15212−15224.

(20) Hamai, S.; Hirayama, F. *J. Phys. Chem.* **1983**, *87*, 83−89.

(21) Roussilhe, J.; Paillous, N. *J. Chim. Phys.* **1983**, *80*, 595−602.

(22) "Ground solids" of **I1**−**I6** were prepared by grinding in a mortar for more than 5 min in the air. Observed PL peaks (solid quantum yields) are 436 nm (0.13) for **I1**, 572 nm (0.02) for **I2**, 591 nm (0.02) for **I3**, 450 nm (0.05) for **I4**, 463 nm (0.15) for **I5**, and 472 nm (0.15) for **I6**. While imides **I1** and **I4**−**I6** have relatively high TL durability, π-elongated thienyl derivatives **I2** and **I3** show decrease of TL activity upon continuous grinding. To regenerate the TL active surfaces and PL performance, organic solvents such as acetone or dichloromethane were added to the sample tubes.

(23) Carbazole derivatives show high potentials in the field of TL and its application. (a) Inoue, T.; Tazuke, S. *Chem. Lett.* **1981**, 589−592. (b) Kitamura, N.; Saravari, O.; Kim, H.-B.; Tazuke, S. *Chem. Phys. Lett.* **1986**, *125*, 360−363. (c) Xu, S.; Liu, T.; Mu, Y.; Wang, Y.-F.; Chi, Z.; Lo, C.-C.; Liu, S.; Zhang, Y.; Lien, A.; Xu, J. *Angew. Chem., Int. Ed.* **2015**, *54*, 874−878.

(24) "Mechanochromic luminescence", which represents the PL controlled by the mode of molecular arrangements and/or conformation, is complementary to TL(ML) studies in stimuli response chemistry and one of the hot and rapidly expanding research fields. (a) Sagara, Y.; Kato, T. *Nat. Chem.* **2009**, *1*, 605−610. (b) Mutai, T.; Satou, H.; Araki, K. *Nat. Mater.* **2005**, *4*, 685−687. (c) Sagara, Y.; Mutai, T.; Yoshikawa, I.; Araki, K. *J. Am. Chem. Soc.* **2007**, *129*, 1520−1521. (d) Kwon, M. S.; Gierschner, J.; Yoon, S.-J.; Park, S. Y. *Adv. Mater.* **2012**, *24*, 5487−5492. (e) Mizoshita, N.; Tani, T.; Inagaki, S. *Adv. Mater.* **2012**, *24*, 3350−3355. (f) Teng, M.-J.; Jia, X.-R.; Yang, S.; Chen, X.-F.; Wei, Y. *Adv. Mater.* **2012**, *24*, 1255−1261. (g) Kunzelman, J.; Kinami, M.; Crenshaw, B. R.; Protasiewicz, J. D.; Weder, C. *Adv. Mater.* **2008**, *20*, 119−122. (h) Chi, Z.; Zhang, X.; Xu, B.; Zhou, X.; Ma, C.; Zhang, Y.; Liu, S.; Xu, J. *Chem. Soc. Rev.* **2012**, *41*, 3878−3896. (i) Mei, J.; Hong, Y.; Lam, J. W. Y.; Qin, A.; Tang, Y.; Tang, B. Z. *Adv. Mater.* **2014**, *26*, 5429−5479.

(25) Frisch, M. J.; Trucks, G. W.; Schlegel, H. B.; Scuseria, G. E.; Robb, M. A.; Cheeseman, J. R.; Scalmani, G.; Barone, V.; Mennucci, B.; Petersson, G. A.; Nakatsuji, H.; Caricato, M.; Li, X.; Hratchian, H. P.; Izmaylov, A. F.; Bloino, J.; Zheng, G.; Sonnenberg, J. L.; Hada, M.; Ehara, M.; Toyota, K.; Fukuda, R.; Hasegawa, J.; Ishida, M.; Nakajima, T.; Honda, Y.; Kitao, O.; Nakai, H.; Vreven, T.; Montgomery, J. A., Jr.; Peralta, J. E.; Ogliaro, F.; Bearpark, M. J.; Heyd, J.; Brothers, E. N.; Kudin, K. N.; Staroverov, V. N.; Kobayashi, R.; Normand, J.; Raghavachari, K.; Rendell, A. P.; Burant, J. C.; Iyengar, S. S.; Tomasi, J.; Cossi, M.; Rega, N.; Millam, N. J.; Klene, M.; Knox, J. E.; Cross, J. B.; Bakken, V.; Adamo, C.; Jaramillo, J.; Gomperts, R.; Stratmann, R. E.; Yazyev, O.; Austin, A. J.; Cammi, R.; Pomelli, C.; Ochterski, J. W.; Martin, R. L.; Morokuma, K.; Zakrzewski, V. G.;

DOI: 10.1021/acs.joc.5b02191
J. Org. Chem. 2016, 81, 433−441

Voth, G. A.; Salvador, P.; Dannenberg, J. J.; Dapprich, S.; Daniels, A. D.; Farkas, O.; Foresman, J. B.; Ortiz, J. V.; Cioslowski, J.; Fox, D. J. *Gaussian 09*, Revision A.02; Gaussian, Inc.: Wallingford, CT, 2009.
(26) Kitagawa, T.; Matsubara, H.; Okazaki, T.; Komatsu, K. *Molecules* **2014**, *19*, 15298−15313.
(27) Zimmer, H.; Barcelon, M. A.; Jones, W. R. *J. Organomet. Chem.* **1973**, *63*, 133−138.
(28) Weisemann, C.; Schmidtberg, G.; Brune, H.-A. *J. Organomet. Chem.* **1989**, *361*, 299−308.
(29) SHELXT Version 2014/4: Sheldrick, G. M. *Acta Crystallogr., Sect. A: Found. Crystallogr.* **2014**, *70*, C1437.
(30) Sheldrick, G. M. *Acta Crystallogr., Sect. A: Found. Crystallogr.* **2008**, *64*, 112−122.

DOI: 10.1021/acs.joc.5b02191
J. Org. Chem. 2016, 81, 433−441